Available online at www.sciencedirect.com
SCIENCE DIRECT
European Journal of Pharmaceutics and Biopharmaceutics 60 (2005) 401–406
European Journal of Pharmaceutics and Biopharmaceutics
www.elsevier.com/locate/ejpb

Research paper

Two-month ciprofloxacin implants for multibacterial bone infections

C. Castro[b], C. Évora[a], M. Baro[c], I. Soriano[a], E. Sánchez[a,*]

[a]*Departamento de Ingeniería Química y Tecnología Farmacéutica, Facultad de Farmacia, Universidad de La Laguna, Tenerife, Spain*
[b]*Servicio de Farmacia, Grupo Hospitén S.L., Tenerife, Spain*
[c]*Servicio de Traumatología, Hospitén Rambla S.L., Tenerife, Spain*

Received 3 August 2004; accepted in revised form 1 February 2005
Available online 5 April 2005

Abstract

A ciprofloxacin implant formulation composed of 12% hydroxyapatite, 36% tricalcium phosphate, 12% poly(DL-lactide) (PLA) and 40% ciprofloxacin was characterized in vivo for use in treatment of multibacterial bone infection. After the implant was inserted in the femur of rabbits, approximately 90% of the total ciprofloxacin was released within 8 weeks, maintaining therapeutic levels in the femur and tibia. Throughout the femoral cortex and marrow these remained higher than the minimum inhibitory concentrations (MIC) against the most common pathogens causing osteomyelitis. Levels in tibia cortex were also above MIC for 6 weeks. The implant was characterized in terms of polymer degradation and morphological and crystallographic changes. X-ray analyses confirmed the osteoconductivity and biocompatibility of these materials. The sequential changes in the femur were those of a normal surgical trauma reaction followed by a repair process. All the results confirmed that ciprofloxacin release is limited by its low solubility, and that implant erosion and bone ingrowth into the implants enhance the antibiotic release.

Keywords: Ciprofloxacin implants; Bone infection; Biocompatibility; Calcium phosphates; Poly(lactic acid)

1. Introduction

Ciprofloxacin (CFX) is currently the most widely used fluoroquinolone for bacterial bone infection, since its MIC is low (0.25–2 μg/ml) for most of the pathogens that cause osteomyelitis, such as *Staphylococcus aureus*, *Staphylococcus epidermis*, *Pseudomonas aeruginosa* and *Proteus mirabilis* [1,2]. However, complicated infections with multiple organisms including Gram-negative bacilli frequently occur [1], requiring higher and more prolonged concentrations. Therefore, the advantages of local antibiotic administration—high local levels with low systemic toxicity—are nowadays recognized. Some important results have shown the potential effectiveness of quinolones in local drug delivery systems designed to treat bone infection, using carriers such as hydroxyapatite–anionic collagen composite [3] and biodegradable polymers [4–9], or a calcium phosphates and biodegradable polymer mixture [10].

The aim of this work was to test the bone antibiotic concentration achieved after the insertion of a CFX implant to treat complicated multi-organism bone infections, which require a high antibiotic concentration in bone for long periods. For this, the implants were characterized in terms of antibiotic release kinetics, morphology and changes in component properties, bone CFX levels, biocompatibility and osteoconductivity. This study was carried out with a CFX implant composed of 12% hydroxyapatite, 36% tricalcium phosphate, 12% poly(DL-lactide) (PLA) and 40% CFX, selected from nine formulations compared to monitor the influence of different factors on the release kinetics [10].

2. Materials and methods

2.1. Implants preparation

The implants were prepared as previously described [10] using Resomer® R203 (PLA, weight-average molecular

* Corresponding author. Departamento de Ingeniería Química y Tecnología Farmacéutica, Facultad de Farmacia, Universidad de La Laguna, 38200 La Laguna, Tenerife, Spain. Tel.: +34 922 318 509; fax: +34 922 318 506.
E-mail address: esanchez@ull.es (E. Sánchez).

0939-6411/$ - see front matter © 2005 Elsevier B.V. All rights reserved.
doi:10.1016/j.ejpb.2005.02.005

weight, $M_w = 28.8 \pm 0.235$ kDa, polydispersity, pd = 1.53 ± 0.014), supplied by Boehringer Ingelheim KG (Germany), tricalcium phosphate powder (TCP) and hydroxyapatite powder (HAP) purchased from Panreac and Osteosyn (Spain), respectively, and CFX kindly provided by Bayer (Spain). Briefly, a 500 mg powder mix of 12% PLA, 48% hydroxyapatite/tricalcium phosphate (25/75) and 40% CFX was compressed using a 6 mm punch in a Carver hydraulic press at room temperature and 320 MPa for 5 min, to obtain $9.4(\pm 0.034) \times 6.0(\pm 0.005)$ mm cylindrical implants with a mean weight of 500.5 ± 1.6 mg.

2.2. Surgical procedure and sampling schedule

The local committee for animal studies at the University of La Laguna had previously approved animal experiments. All experiments comply with the E.C. Guideline (86/609/CEE) on care and use of animals in experimental procedures.

Male New Zealand rabbits, weighing 3–4 kg, were anaesthetized with ketamine (35 mg/kg) and xylazine (5 mg/kg). A vertical external parapatellar incision was made in the right knee and a hole in the intercondylar space was made with a 6 mm Shannon burr, then the implant was gently inserted into the marrow cavity of the femur as previously described [11]. SC injections of buprenorphine (25 μg/kg) were administered before surgical operation and every 12 for 72 h, to minimize pain. After recovering from anaesthesia, the animals were allowed free movement in their cages.

After insertion of one implant in the right femurs of 24 rabbits, four rabbits were sacrificed at 1, 2, 4, 6, 7 and 8 weeks. The femurs and tibias were extracted and the implants removed. The femurs and tibias were divided into five and three pieces, respectively, and then the cortex and bone marrow were separated and incubated several times in citrate buffer pH 4.0, with shaking for 24 h to total extraction.

Three of the four implants extracted at each time-point were incubated in citrate buffer as above for CFX extraction. The fourth implant was kept for characterization in terms of morphology, crystallographic properties, and polymer molecular weight.

Blood samples were extracted weekly from the marginal vein and frozen until their CFX levels were analyzed. Before blood extraction, rabbit weight and temperature were recorded; both stayed within the normal range during the experiments.

CFX levels in serum, bone tissues and implants were evaluated by microbiological assays [10].

X-rays were taken of each rabbit at 2 days, then 6 and 8 weeks after implantation using Phillips Optimus X-ray equipment set at 44 kV, 3.6 mA/s and 15.4 mSv with the rabbits restrained in the posterior–anterior and lateral positions.

3. Implant characterization

3.1. In vitro release assay

Release of CFX from the implants was assayed spectrophotometrically at 277 nm in triplicate under sink conditions at 37 °C in isotonic phosphate buffer solution (pH 7.4).

3.2. Water uptake and mass loss

These assays were carried out as previously described [10]. Briefly, the implants were weighed before and after incubation in the release medium and the final weights were recorded after drying over phosphorus pentoxide. The mass loss was calculated taking into account the CFX already released.

3.3. Porosity

After each time interval, samples from six implants were tested for porosity during the in vitro release assays, using a mercury penetration porosimeter (Micromeritics Pore Sizer 9305, USA).

3.4. Implant morphology

Scanning electron microscopy (SEM, Jeol JSM-6300) at 15 kV was used to characterize the implant structures (cross-section and surface) periodically during the in vitro and in vivo release assays. The dried samples were coated with gold–palladium under an argon atmosphere.

3.5. Crystallographic structure

Compound crystallographic structure was determined by X-ray diffraction (XRD, Phillips X'pert, graphite-monochromated Cu Kα radiation, $\lambda = 1.5418$ Å). Patterns for

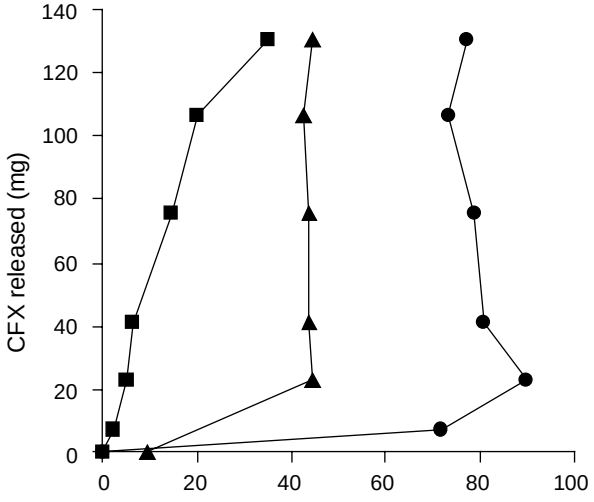

Fig. 1. Effect of percentage mass loss (■), porosity (▲) and water uptake (●) on in vitro CFX release from implants.

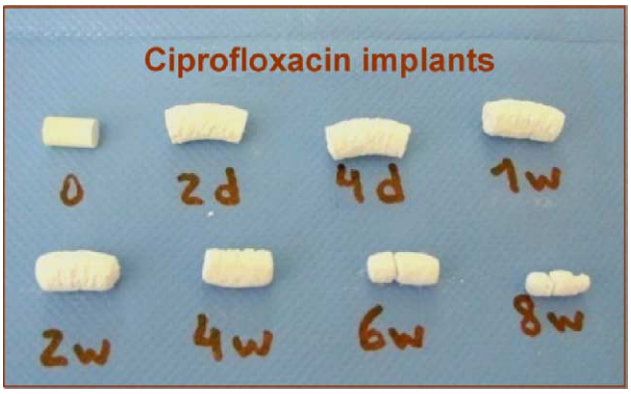

Fig. 2. Morphological evolution of the implants during in vitro release.

phase identification were collected with a scanning step of 0.02° in 2θ over the angular range $0 < 2\theta \leq 80°$ with a collection time of 3 s per step.

3.6. Polymer degradation

To study the implant polymer degradation during the release assay, dried samples were analyzed after each time interval by differential scanning calorimetry (DSC) and gel permeation chromatography (GPC). The DSC profiles of PLA were obtained from milled implants heated at 10 °C/min (DSC 821, Mettler, Toledo) in a nitrogen atmosphere. Average molecular weights were periodically determined by GPC using a Waters® chromatograph with one Model 510 pump, Rheodyne injector, Model 410 differential refractive index detector, an oven for columns and Maxima 820 chromatography software v.3.30 for data acquisition. Three columns (Styragel® HR4, HR3 and HR1) were used at 31 °C, with tetrahydrofuran (THF, Merck) at a flow rate of 1 ml/min. To calibrate the system, polystyrene monodisperse standards were used (Tokyo Soda Ltd). The PLA in the dried implant samples was dissolved in THF and then filtered before injection.

4. Results and discussion

The in vitro release curve obtained with the CFX implants chosen for the present study showed that 40% of total CFX was released in 4 weeks and more than 90% in approximately 4 months. The previous results already showed that CFX within the implants swelled immediately after incubation and the percentage release rate decreased proportionally to compression pressure, PLA/phosphates ratio and drug loading [10].

Implant behaviour in the release medium in terms of water uptake, porosity and mass loss is shown in Fig. 1.

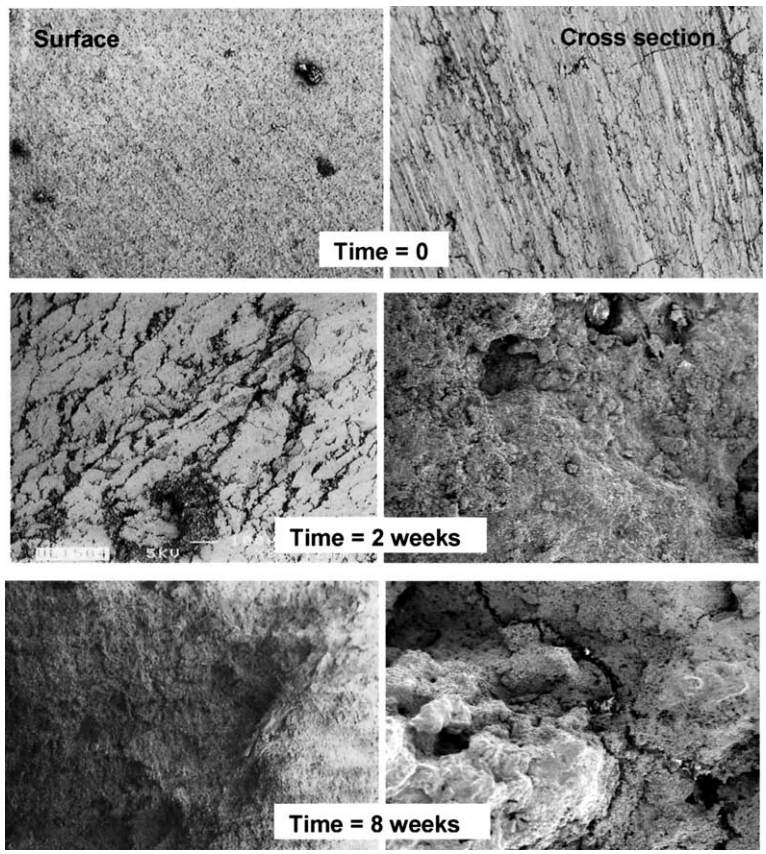

Fig. 3. Scanning electron micrographs of implant surface and cross-sections at time 0; cross-sections after 2 and 8 weeks of in vitro release (left) and implantation in rabbit femur (right).

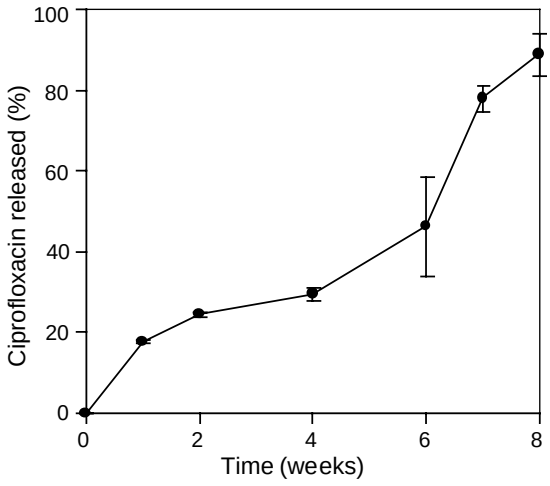

Fig. 4. CFX release profile from implants after insertion in the femurs.

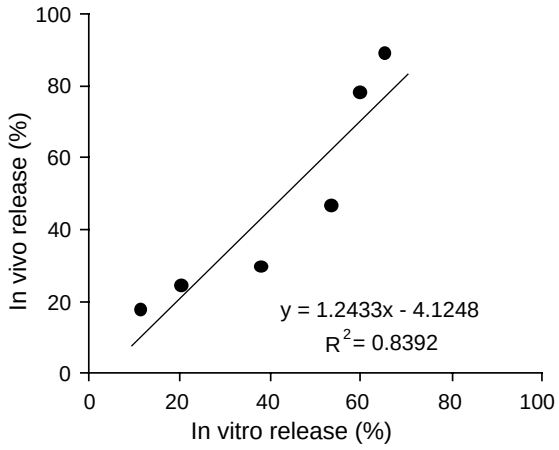

Fig. 5. In vitro–in vivo CFX release correlation.

The intramatrix pressure caused by CFX hydration-swelling led to an increase in porosity during the first week. Afterwards, hydration and porosity stayed constant, whereas the mass loss increased throughout the release assay. Therefore, release depends on the erosion and disintegration of the device, since CFX is poorly water-soluble and the increased surface area enhances drug solubility/release. Visual observation (Fig. 2) shows the swelling and disintegration, and SEM pictures (Fig. 3) the external surface cracks caused by the CFX swelling, which aid in further erosion and progressive external mass loss. In addition, the T_g and molecular weight of PLA in the matrix did not change during the release assay. Actually, the PLA contributed a certain plasticity that delayed the erosion–disintegration of the implant, lowering the release rate with respect to implants made with only phosphates, as previously described [10]. All these results confirm that the low aqueous solubility of CFX plays a dominant role in the drug release mechanism.

Despite the slow in vitro release, the formulation was tested in rabbits since according to our previous paper the in vivo release rate of CFX from PLA/phosphate implants is approximately double that in vitro [10], so this formulation was expected to extend in vivo release by about two months, maintaining a high antibiotic concentration in the bone, highly appropriate for preventing and treating multibacterial infection. In fact, the in vivo release profile was characterized by a slower initial phase of 4 weeks, afterwards faster than in vitro. Approximately 90% of the antibiotic was released in 8 weeks (Fig. 4), and the in vivo–in vitro correlation (Fig. 5) showed a slope higher than one due to the faster in vivo release.

Fig. 6 shows CFX concentrations in the different areas of the femur versus time, together with the MIC values for *S. aureus*, *S. epidermidis*, *Escherichia coli*, *P. aeruginosa* and *P. mirabilis*. The highest levels were achieved in the distal metaphysis and diaphysis of the femur, the zones closest to the implant. However, the cortex and bone

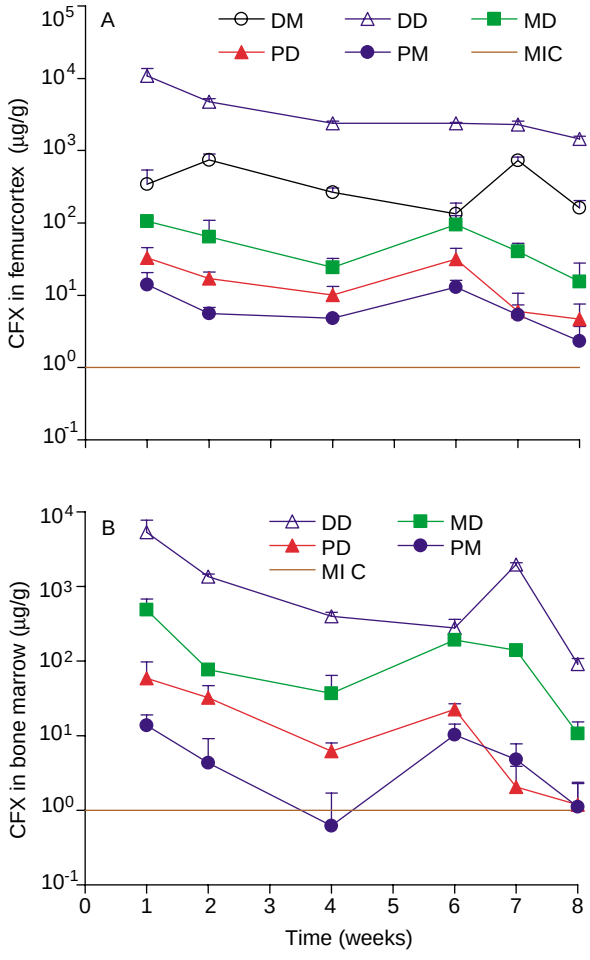

Fig. 6. CFX concentrations achieved in the different areas of the femur cortex (A) and the bone marrow (B) after implantation: distal metaphysis (DM), distal diaphysis (DD), medial diaphysis (MD), proximal diaphysis (PD), proximal metaphysis (PM) and minimum inhibitory concentration (MIC).

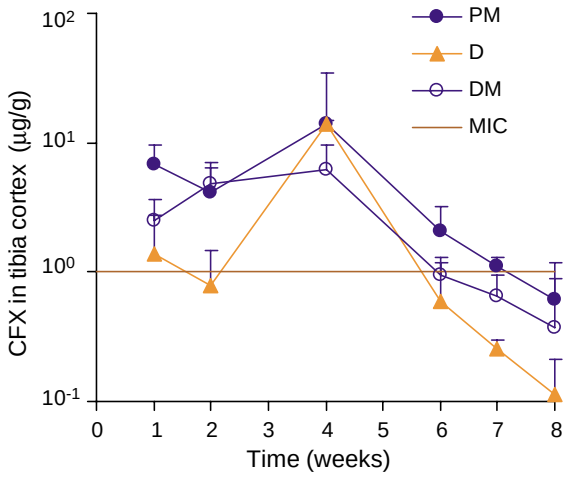

Fig. 7. CFX concentrations achieved in the different areas of the tibia cortex after implantation: proximal metaphysis (PM), diaphysis (D), distal metaphysis (DM) and minimum inhibitory concentration (MIC).

marrow curves were different. The cortex profile showed a prolonged plateau in all the sampled areas, while the marrow profile was irregular during the same 8-week period. This was also the case with the tibia cortex (Fig. 7), which showed a major decrease after the fourth week. The tibia marrow and plasma samples were evaluated regularly, but the concentrations were non-detectable.

With regard to therapeutic efficiency, antibiotic concentrations achieved in the femoral cortex and marrow and even the tibia cortex were found to be higher than the MIC for *S. aureus*, *S. epidermidis*, *E. coli*, *P. aeruginosa* and *P. mirabilis*, although not in the tibia marrow. Therefore, therapeutic coverage in the femur and tibia is warranted for at least 8 and 6 weeks, respectively. These bone concentrations are higher and cover all along the femur for longer than those previously reported using polyglycolic acid implants [8]. Although the bone CFX levels may be comparable to those reported for poly(lactide-*co*-glycolide) acid [9], the concentration profiles are completely different. Their results show levels lower than in the present study during the first 4 weeks, whereas after the fifth week they report an increase. In addition, they tested the CFX levels for 6 weeks in the total femur tissue rather than cortex and bone marrow separately, observing high concentration variability. Clearly, to treat bone infection, an aggressive antibiotic treatment is desirable, high therapeutic levels in most of the bone should be achieved as soon as possible and kept up.

To illustrate changes in radiographic findings, the images obtained of one animal are shown as example in Fig. 8, revealing a progressive regenerative bone response after implantation, beginning with a normal surgical trauma reaction and followed by a repair process surrounding the implant with mature bone tissue. After 48 h, a radiolucent area (due to the insertion aperture) was observed, with soft tissue deformation attributable to surgical trauma around the implant, and the cortices were clearly differentiated. At 6 weeks, implant density appeared very similar to that of the surrounding bone, although the periphery was less dense than the central area. The images show interconnection between implant and femur with bone spiculatae visibly penetrating the implant, fusion with the posterior cortex, and bone neoformation in the proximal area, all evidence of near-definitive bone repair. Gradual implant disintegration was also observed, with greatly reduced density in the peripheral area of the implant and loss of general integrity at 8 weeks. X-ray imaging clearly showed mature bone formation around the implant, with the implant density similar to the surrounding bone. Clearly, the implant inserted in the femur was invaded by new bone tissue and there were no periosteal reactions, indicating absence of infection and inflammatory reaction during the experiment. This confirms the osteoconductive properties and biocompatibility of this implanted delivery system, respectively.

To elucidate the in vivo release mechanism, the implants were characterized after extraction from the femur. The SEM results (Fig. 3) showed great internal erosion during the in vivo experiments that could partially explain the faster in vivo release than in vitro. The images showed cracks in the external surface of the implants (also seen in cross-section images), which aid further erosion. In the in vitro study, the CFX within the implant absorbs water and swells in volume, initiating the erosion. The same hydrated form of CFX already observed by XDR [10] also appears in the implant diffraction pattern obtained 1 week after implantation, where only the peak corresponding to the hydrated CFX at 6.87° (2θ) was visible (Fig. 9). In addition, after 8 weeks, the PLA molecular weight dropped slightly from 28.8 kDa initially to 24.5 and the T_g stayed around

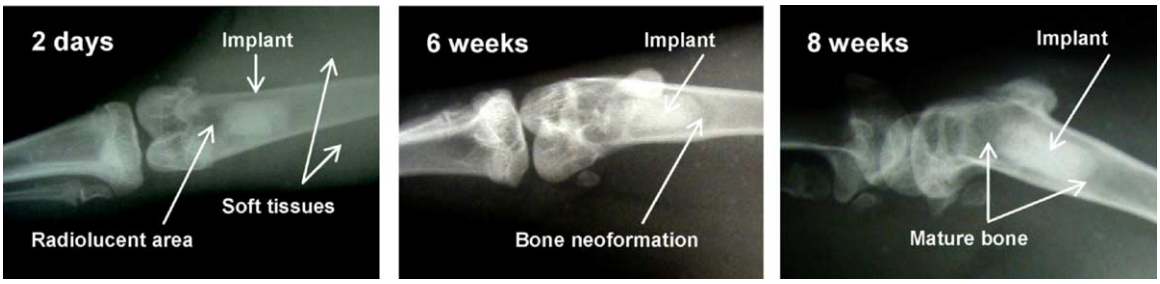

Fig. 8. Sequential radiographic images after implantation in rabbit femur at 2 days, and at 6 and 8 weeks.

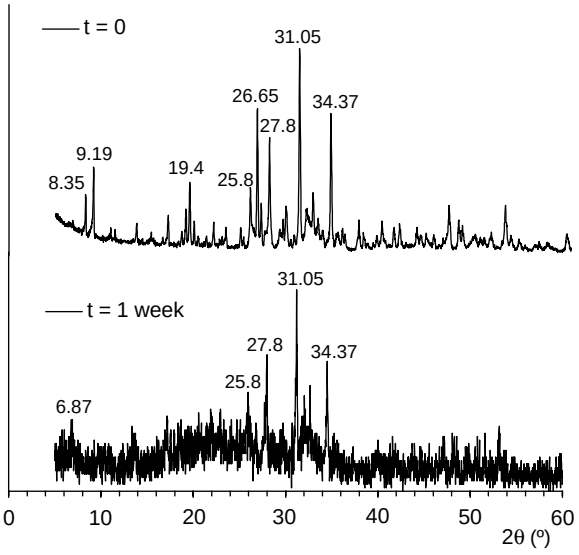

Fig. 9. X-ray diffraction pattern of ciprofloxacin implants at time 0 and 1 week after implantation in rabbit femur. The peaks at 8.35, 9.19, 19.4 and 26.65° (2θ) correspond to CFX, those at 25.8, 27.8, 31.05 and 34.37° (2θ) correspond to tricalcium phosphate.

the initial value of 43.8 °C, indicating no significant degradation.

These results confirm that aqueous CFX solubility governs release and therefore, erosion/disintegration processes are necessary for total release. However, the osteoconductivity of the materials used in the delivery system facilitates bone tissue ingrowth and vascular network formation within the system, further contributing to erosion and thus enhancing antibiotic release. A favourable implant-blood gradient is created, draining away most of the remaining antibiotic which leaves the implant via general blood circulation. Therefore, less antibiotic is available to diffuse into the tibia, explaining the reduced CFX concentration in tibia after 4 weeks.

In conclusion, this implant system promises high efficacy in treating bone multi-infections, since therapeutic concentrations are maintained in the bone itself over a long period of time, confirming the benefits of local drug delivery.

Acknowledgements

The authors thank the Radiography Service of Hospiten Rambla S.L. for the X-ray images. This work was supported by the CICYT as part of Project SAF 98-0167, Ministry of Education and Science, Spain.

References

[1] E.P. Armstrong, V.A. Elsberry, Bone and joint infections in: J.T. Dipiro, R.L. Talbert, G.C. Yee, G.R. Matzke, B.G. Wells, L.M. Posey (Eds.),, Pharmacotherapy. A Pathophysiologic Approachthird ed., Aappleton and Lange, Stamford, CT, 1997, p. 111.
[2] H.P. Lambert, F.W. O'Grady, Quinolones in: H.P. Lambert, F.W. O'Grady (Eds.),, Antibiotic and Chemotherapysixth ed., Churchill Livingstone, Edinburgh, 1992.
[3] V.C. Martins, G. Goissis, Nonstoichiometric hydroxyapatite–anionic collagen composite, a support for the double sustained release of gentamicin and norfloxacin/ciprofloxacin, Artif. Organs 24 (2000) 224–230.
[4] C. Désévaux, V. Lenaerts, C. Girard, P. Dubreuil, Characterization of crosslinked high amylose starch matrix implants. 2. In vivo release of ciprofloxacin, J. Control Release 82 (2002) 95–103.
[5] K. Kanellakopoulou, E.J. Giamarellos-Bourboulis, Carrier systems for the local delivery of antibiotics in bone infections, Drugs 59 (2000) 1223–1232.
[6] D.P. Nicolau, L. Nie, P.R. Tessier, H.P. Kourea, C.H. Nightingale, Prophylaxis of acute osteomyelitis with absorbable ofloxacin-impregnated beads, Antimicrob. Agents Chemother. 42 (1998) 840–842.
[7] L. Nie, D.P. Nicolau, P.R. Tessier, H.P. Kourea, B.D. Browner, Use of bioabsorbable polymer for the delivery of ofloxacin during experimental osteomyelitis treatment, J. Orthop. Res. 16 (1998) 76–79.
[8] J.P. Overbeck, S.T. Winckler, R. Meffert, P. Törmälä, H.U. Spiegel, E. Brug, Penetration of ciprofloxacin into bone: a new bioabsorbable implant, J. Invest. Surg. 8 (1995) 155–162.
[9] M. Ramchandani, D. Robinson, In vitro–in vivo release of ciprofloxacin from PLGA 50:50 implants, J. Control Release 54 (1998) 167–175.
[10] C. Castro, E. Sánchez, A. Delgado, I. Soriano, P. Núñez, M. Baro, A. Perera, C. Évora, Ciprofloxacin implants for bone infection. In vitro–in vivo characterization, J. Control Release 93 (2003) 341–354.
[11] M. Baro, E. Sánchez, A. Delgado, A. Perera, C. Evora, In vitro–in vivo characterization of gentamicin bone implants, J. Control Release 83 (2002) 353–364.